DOI 10.18524/1810-4215.2022.35.268006

PROTOPLANETARY DISKS AROUND CLASSICAL T TAURI STARS

N. Z. Ismailov[1], U. S. Valiev[2], N. S. Dzhalilov[1]

[1] Shamakhy Astrophysical Observatory named after N. Tusi of the National Academy of Sciences of Azerbaijan, Shamakhy, Azerbaijan, AZ 5626, *ismailovnshao@gmail.com*

[2] Batabat Astrophysical Observatory, Nakhichevan Branch of the National Academy of Sciences of Azerbaijan, Nakhichevan, Azerbaijan, *veliyev_ulvu@mail.ru*

ABSTRACT. We have studied the energy distribution curves for a statistically significant number of classical T Tauri stars. It is shown that out of 49 stars, only 7 (14%) has I type of spectrum distribution, the rest belong to type II. Fundamental parameters, including the mass and age of objects are determined. It is shown that the amount of excess radiation in the far IR range increases with age. The change in mass with age, in contrast to Herbig's AeBe stars, exhibits a complex character.

Keywords: Pre-Main sequence stars, circumstellar disks, energy distribution, evolution.

АНОТАЦІЯ. Зорі типу T Tau зазвичай можна виявити поруч із молекулярними хмарами та ідентифікувати за їх змінністю (дуже нерегулярною) в оптичному діапазоні та хромосферній активності. Більше половини зорь типу T Tau мають навколозоряний диск, який можна назвати протопланетним. Цей диск розсіюється за 10 млн років, частково випадаючи на зорю завдяки акреції, частково витрачаючись на формування планет і частково видуваючись зоряним вітром. Більшість зорь типу T Тельця є членами подвійних систем.

У цій роботі ми вивчили криві розподілу енергії для статистично значущої кількості класичних зір типу T Тельця. Показано, що з 49 зір лише 7 (14%) мають I тип розподілу спектра, інші відносяться до II типу. Визначено основні параметри, у тому числі масу та вік об'єктів. Показано, що з віком збільшується кількість надмірного випромінювання у далекому ІЧ-діапазоні. Зміна маси із віком, на відміну зір AeBe Хербіга, носить складний характер.

Ключові слова: попередні зорі головної послідовності, навколозоряні диски, розподіл енергії, еволюція.

1. Introduction

T Tauri type stars (TTS) are low mass ($M \leq 2\ M_\odot$) and have 1–15 Myr ages, have just emerged from their dust cocoon and they are in the Pre-Main Sequence (PMS) stage of evolution. TTSs are formally divided into two subclasses: the so-called classical T Tauri (CTTS) stars are surrounded by an optically thick circumstellar accretion disks. T Tauri stars with weak emission lines in the spectrum and with the partially dissipated residual circumstellar disks are named (WTTS) (Bouvier et al., 2007, Appenzeller & Mundt, 1989, Petrov, 2021). Historically, the strength of the equivalent width (EW) of the Hα emission line, equal to 10 Å, was proposed as the boundary between the CTTS and WTTS groups. However, since most WTTS show Hα emission also due to the chromospheric activity, it is problematic to establish a precise observational boundary between WTTS and CTTS. Later, it was shown that the width of the Hα emission line measured at the level of 10% of the peak intensity (hereinafter, Hα10%) and the Hα profile measured in high-resolution spectra are more sensitive diagnostics of accretion than the EW of the Hα line obtained from spectral data with low resolution (Mamajek et al., 2009). Non-accreting objects exibite narrow ($\Delta V \lesssim$ 230–270 km s^{-1}) and symmetric line profiles of chromospheric origin, while accreting objects has wide ($\Delta V \gtrsim$ 230–270 km s^{-1}) and asymmetric profiles (Ribas et al., 2014, Williams and Cieza, 2011).

It is known that planets are formed in gas- and dust-rich circumstellar disks of young stars. Therefore, the study of the physical properties and evolutionary mechanisms of protoplanetary disks in young stars is important for understanding of the planet formation processes. Various studies have shown that the typical dissipation time scale for protoplanetary disks is about 3 Myr (e.g., Mamajek et al., 2009; Ribas et al. 2014), and the oldest disks are typically up to 16 Myr old (Pollak et al. 1996). The evolution of circumstellar disks from the initial reservoir of the interstellar medium, the gas and dust mixture, towards planetary systems is occured by the growth of dust grains, viscous spreading and accretion onto the central star (or onto the forming protoplanets) and dissipation of the initial gas (Williams & Cieza, 2011). Although a large number of direct images and high-resolution spectroscopic data have been collected over the past decades, the various stages of disk evolution remains poorly distinguished for observations (Wyatt et al. 2015).

Our previous studies shows that the properties of disks apound individual stars of WTTS coincide with those of CTTS, and different populations with residual disks are distinguished, which can exhibit the stages of evolution between them (Ismailov & Valiyev, 2022a). It is assumed that when the primary disk is completely dissipated, the final stage of evolution will be characterized by residual disks, and/or will assemble into

planetesimals and planets. Collisions between planetary remnants or cometary evaporation can produce a second generation of the dust (Hughes et al. 2018). Studies of the dust mass distribution show their significant differences in various young clusters (see, for example, Villenave et al., 2021). These data show that there is a tendency for the dust to decrease in older clusters. According to Manara et al. (2020), even in clusters older than 5 Myr, the observed disk accretion rate is high, and the primary gas-to-dust ratio changes with time in a complex way.

The observed amount of excess radiation in the far-IR spectrum should be proportional to the mass of the dust in the disk. Therefore, the amount of excess radiation in the far-IR range can be an indicator of the amount of dust in the disk. In the present work, we studied the spectral energy distribution curves in the spectral range 0.36–100 μm (SEDs) of a statistically significant amount of CTTS.

2. Observational data

We have selected the program stars from the Herbig & Bell (1988) (HBC) catalogue. We tried to choose such stars for which the emission level in the spectral lines are different. Table 1 lists 49 program stars in ascending order of number in the HBC catalogue. The table 1 lists from left to right in columns: name of the object, the HBC number, the distance to the object, the interstellar extinction coefficient, the spectral types, the effective temperatures adopted to them according to Pecaut et al. (2013), and the main literature sources for each star. These references are given in a separate list in the footnote of the table. All source distances were rechecked and refined using the Gaia DR3 data archive (https://gea.esac.esa.int/archive/). For individual stars, the interstellar extinction coefficients, given in the literature by different authors differ significantly. In such cases, using the B–V color index for normal MS stars, we redefined the value of the parameter Av, assuming that the normal law of interstellar extinction is observed and the extinction coefficient is R=3.1.

Note that the photometric data of the optical and IR ranges collected from the catalogs were obtained non simultaneously; therefore, this can manifest itself as a weak excess IR radiation in the spectral energy distribution (SED) (Strom et al., 1989). In addition, the variability of individual stars can introduce some distortion on the SED curves. Typical brightness variations for TTS in the V band are of the order $\Delta V \approx 0.1$─0.5 mag (Grankin et al., 2007, Herbst&Shevchenko, 1999), so the expected maximum flux change in this band can be about 35%. The maximal variation in the K=2.2 μm band are about $\Delta K \approx 0.3$ mag (Kenyon &Hartmann, 1995), which can provide an error in the fluxes in this band of about 25%.

The procedure of constructing the SED curves for program stars and their approbation for standard stars, as well as the analysis of sources of measurement errors, are described in detail in our previous works (Ismailov, et al. 2021a, Ismailov 2021b, Ismailov & Valiyev 2022).

Table 1: Collected literature data for program stars

Target name	HBC	D, pc	Av	W(Hα) Å	Sp type	Teff K	Reference
LkHa 262	8	246	1.6	31	M0	3850	32, 17, 2
LkHα 271	13	279	4.6	186	K4	4620	2, 8
FM Tau	23	132	0.7	71	M0	3850	10, 9, 30
CW Tau	25	131	2.16	135	K3	4840	27, 10, 44
DD Tau	30	126	1.36	182	M3.5e	3300	10, 27
DG Tau	37	125	0.62	113	K7, K6ve	4050	9, 10,11
DK Tau	45	140	1.4	19	K7e, K8.5	4050	32, 27
XZ Tau	50	147	1.71	274	M2e	3550	27, 30
UZ Tau	52	140	1	80	M1/3Ve	3600	5,25 , 24
GH Tau	55	140	0.25	15	M0.6	3800	5, 26, 27
GK Tau	57	130	0.53	16	K 6.5	4200	1, 2,5
CI Tau	61	160	1.58	102	K7, K5.5	4050	10, 40, 27
DP Tau	70	140	1.22	85	M0.8	3700	30, 27, 9
GO Tau	71	142	2.44	81	M0, M2.3	3850	27, 10, 30
YZ Ori	120	388	0.218	70	K7e	4050	28, 29, 10
KP Ori	124	113	1.2	127	M0	3850	43, 44, 2
AB Ori	135	410	0.81	45	K7	4050	5, 31, 30
CE Ori	152	375	0.496	74	K5e	4450	44, 10
BC Ori	166	304	0.35	151	K7.5e	4000	41, 42
BE Ori	168	398	2.61	68	K0	5280	32, 18, 2

Haro 4-255	176	392	5.0	100	K7:	4780	17, 2, 52
LP Mon	214	830	0.7	58	K7	4050	19, 45, 33
NX Mon	216	706	-2.45	211	K7,M5	3550	50, 38,51
V591 Mon	235	717	0.25	106	K4	4620	33, 38, 39
V 432 MON	237	726	0.4	83	K5	4450	32, 33, 34
RU Lup	251	157	0.37	216	K7 e	4050	6, 21, 22
V 852 Oph	258	131	0.9	167	M0	3850	30, 3, 2
Haro 1-16	268	146	1.38	54	K3e	4840	2, 17
EM*AS209	270	121	1.2	71	K4ve	4620	2, 14, 15
S CrA	286	130	1.92	90	G0Ve	5900	32, 2, 12
FQ Tau	377	140	1	114	M3	3400	35, 32,36
IP Tau	385	129	0.2	11	M0.6	3800	30, 17, 2
FV Tau	386	136	4.73	23	K5	4450	9, 30, 37
Haro 6-13	396	128	2.81	88	M0	3850	9, 30, 17
FZ Tau	402	129	1.83	204	M0	3850	9, 53,
TW Cha	567	183	1	26	K8Ve,	3970	2, 47, 18
TW Hya	568	60	0.27	86	K6, M0	4100	14, 10, 46
Ass Cha T 1-15	574	190	1.55	94	K5Ve	4450	32, 47, 48
WW Cha	580	188	2.31	54	K2	5040	32, 2
Wy cha	583	174	1.65	52	K7-M0	4050	2, 16,17
VW cha	585	168	2.6	116	K8e, K7	3970	10, 20, 13
XX Cha	586	192	1	87	M3e	3500	2, 18,13
Ass cha T1-32	590	188	0.3	32	M0.5e	3800	2, 12, 13
THA 15-5	600	157	2.04	97	K7e	4050	2, 12, 49
HO Lup	612	200	1	220	M1	3680	32, 6,
SZ 102	617	422	0.32	20	K2, K0V	5040	2, 6, 7
SZ 111	622	158	0.5	145	M0	3850	11, 23, 12
AS 205	632	140	1.09	155	K0e, K5e	4500	1, 2, 3
V 1082 Cyg	728	646	0.13	11	K5, K6	4250	2, 4

List of References in the tabl.1:

(1) Zacharias N. et al., 2012yCat, 1322, 0; (2) Cutri R. M. et al., 2003yCat, 2246, 0; (3) Ducourant C. et al., 2005 A&A, 438, 769; (4) Alfonso-Garzón J. et al., 2012 A&A, 548A, 79; (5) Herbig G. H. 1977 ApJ, 214, 747; (6) Hughes J. et al., 1994 AJ, 108, 1071; (7) Merín B. et al., 2008 ApJS, 177, 551; (8) Winston E. et al., 2010 AJ, 140, 266; (9) Audard M. et al., 2007 A&A, 468, 379; (10) Ducati J.R. 2002 yCat.2237, 0; (11) Röser S. et al., 2008 A&A, 488, 401; (12) Cutri R. M. et al., 2014 yCat, 2328, 0 (13) Luhman K.L. 2004 ApJ, 602, 816; (14) Høg E. et al., 2000 A&A, 355L, 27;(15) Salyk C. et al., 2013 ApJ, 769, 21S; (16) Camargo J.I. et al., 2003 A&A, 409, 361; (17) Lasker B.M. et al., 2008 AJ, 136, 735; (18) Tonry J.L. et al., 2018 ApJ, 867, 105; (19) Chambers K.C. et al., 2016 arXiv 161205560; 20) Kirk H., Myers P.C. 2011 ApJ, 727, 64; (21) Bai Yu. et al., 2019 AJ, 158, 93; (22) Bourgés L. et al., 2014 ASPC, 485, 223; (23) Mowlavi N. et al., 2021 A&A, 648, 44; (24) Kraus A.L. Hillenbrand, Lynne A. 2009 ApJ, 704, 531; (25) Bianchi L. et al., 2017 ApJS, 230, 24; (26) Zacharias N. et al., 2009 yCat, 1315, 0; (27) Strom K.M. et al., 1989 AJ 97, 1451; (28) Cohen M., Kuhi L.V.,1979 ApJS, 41, 743; (29) Kounkel M. et al., 2016 ApJ, 821, 8; (30) Lawrence A. et al., 2007 MNRAS, 379, 1599; (31) Frasca A. et al., 2009 A&A, 508, 1313; (32) Sung H. et al., 1997 AJ, 114, 2644S (33) Rebull L.M. et al., 2002 AJ, 123, 1528; (34) Traven G. et al., 2015 A&A, 581, 52; (35) Lucas P.W. et al., 2008 MNRAS, 391, 136; (36) Zhang Z. et al., 2018 ApJ, 858, 41; (37) Luhman K.L. et al., 2010 ApJS, 186, 111; (38) Barentsen G. et al., 2014yCat, 2321, 0; (39) Broos P.S. et al., 2013 ApJS, 209, 32; (40) Torres C.A. et al., 2006 A&A, 460, 695; (41) Wiramihardja S.D. et al., 1991 PASJ, 43, 27; (42) Briceño C. et al., 2019 AJ, 157, 85B; (43) Da Rio, N. et al., 2009 ApJS, 183, 261; (44) Herczeg G.J. Hillenbrand L.A. 2014 ApJ, 786, 97; (45) Dahm S.E., Simon T. 2005 AJ, 129, 829D;(46) Wolf C. et al., 2018 PASA, 35, 10; (47) Frasca A. et al., 2015 A&A, 575A, 4; (48) Stelzer B. et al., 2004 A&A, 423, 1029; (49) Alcalá J.M. et al., 2014 A&A, 561A, 2; (50) Flaccomio E. et al., 2006 A&A, 455, 903; (51) Hsu Wen-Hsin. et al., 2012 ApJ, 752, 59;

3. Obtained results

3.1. SED curves

The constructed SED curves of program stars are shown in Fig. 1. The observational data were approximated by the Castelli & Kurucz (2004) standard stellar models. Since the R, I bands most free of excesses, for the SED curves of CTTS, when fitting with the theoretical curve for stars having the complex spectrum, we focused on these two bands. All SED curves are plotted on the log λ(mkm) ~ log (λF_λ) scale, where λ is the wavelength and F_λ is the absolute radiation flux at the given wavelength. The standard deviation level of points from the approximating curve for the parameter log λF_λ obtained from the SED curves of standard stars was determined as σ=±0.07.

As shown in Ismailov and Valiev (2022), two quantities were used as a measure of excess radiation. The first of them is the difference between the fluxes of the star and the standard in the K band (2.2 μm), i.e., the parameter ΔK. This parameter indicates the excess radiation in the near-IR range (Strom et al., 1989). The second parameter was used by us for the integral excess radiation, and it can be used to measuring both in the UV (denoted as S(UV)), and in the far IR range of the spectrum (signed as S(İR)) (Ismailov and Valiev (2022)). To calculate the integral excess radiation in the spectral region $\lambda_2 - \lambda_1$ (where $\lambda_2 > \lambda_1$), one can apply the expression

$$S = \int_{\lambda_1}^{\lambda_2} log \frac{F_*}{F_m} d\lambda \qquad (1)$$

Here λ_1 and λ_2 are the initial and final wavelengths of the excess radiation region, F_* and F_m are the radiation fluxes of the star and the standard in this region of the spectrum. Obtained values of S(UV) and S(IR) characterise the integral value of excess radiation in the UV and IR ranges of the spectrum (see Fig. 4 in Ismailov and Valiev, 2022). All calculated parameters of excess radiation are given in Table 2.

One of the indicators of the existence of the disk accretion is the absolute luminosity in the Hα emission line. Following to Corcoran & Ray (1998), to calculate the luminosity of stars in the Hα (LHα) line the following relation was used:

$$L_{H\alpha} = 4\pi d^2 F_R W_{H\alpha} \qquad (2)$$

where Table 1 d is the distance of the star, F_R is the absolute flux density in the photometric band R ($\lambda_{eff} \approx$ 7000 Å), WHα is the equivalent width of the Hα line, expressed in angstroms. Using expression (2) for program stars, the logarithm of the luminosity of radiation in the Hα line was calculated in units of the solar luminosity.

Figure 2 shows graphs, dependences of parameters ΔK ~ S(IR), S(UV) ~ S(IR), ΔK ~ log (LHα/$L_\odot$), and S(UV) ~ log (LHα/$L_\odot$). There is a correlation between the parameters ΔK ~ S(IR), in the order r = 52±2%. On the remaining graphs, there is no clear correlation between the corresponding parameters. The excess radiation index ΔK in the near-IR range is an indicator of the disk accretion. The lack of correlation between the parameters ΔK~ log (LHα/$L_\odot$) indicates that the luminosity in the Hα line is formed by various mechanisms, not only by accretion, but also, for example, by chromospheric activity.

To classify the SED curves of program stars, we used the value of the parameter α, obtained from expression:

$$\alpha = \frac{\log\lambda_2 F_2 - \log\lambda_1 F_1}{\log\lambda_2 - \log\lambda_1} \qquad (3),$$

which was proposed by Lada (1987). Here λ_1 and λ_2 ($\lambda_2 > \lambda_1$) are the wavelengths of the corresponding to range on the SED curves, and F_1 and F_2 are the absolute radiation fluxes corresponding to these wavelengths. The parameter α determines the degree of slope of the given section on the SED curve. Our measurements for the region λ_1=2.2 μm and λ_2=12 μm showed that out of 49 stars, only 7 (about 14%) are corresponding to type I spectrum, and the rest have type II spectrum. The results of this classification are presented in Table 2.

3.2. Physical parameters of program stars

First of all, based on the V values cleared of the interstellar reddening, the distance to the star, and the bolometric corrections taken from Pecaut & Mamajek (2013), we have calculated the absolute bolometric stellar magnitudes Mv. Knowing the absolute luminosity of the Sun $Mv_\odot$=4.83 mag, we calculated the absolute luminosities of stars in units of solar luminosity $L/L_\odot$. Further, knowing the effective temperatures T_{eff} and luminosities, we calculated the radiuses of the stars in units of the solar radius $R/R_\odot$. The solar effective temperature $T_\odot$ was taken equal to 5800 K.

Using theoretical evolutionary tracks of Siess et al., (2000), the masses and ages of stars were also determined. The position of stars in the H–R diagram is shownig (Fig. 3) that the masses of program stars are within $0.3 \leq M/M_\odot \leq 2.5$. All calculated parameters are given in the corresponding columns of the Table 2.

To comparison of the masses of program stars obtained in this work with the literature data, on the left panel of the Fig.4 have shown the corresponding diagram. As can be seen, our data are consistent satisfactorily with the literature data. The second panel on the right shows the age-mass dependence in the scale log t ~ M/M⊙ for program stars. As can be seen, no definite regularity is revealed in the distribution of stellar masses by age.

3.3. Spectral type – age relation

In the left panel of the Fig. 5, shown a diagram of the distribution of the parameter's value α with a step 0.25 for program stars. The ordinate shows the percentage ratio of the number of stars Ni to the total number of samples N for a given range of values of the parameter α. As can be seen from this, the largest number of stars (32.5%) have the parameter between $-1.0 \leq \alpha < -0.5$, and in general, the shape of the distribution is close to the normal distribution.

The second panel in Fig. 5 shows the dependence of the average value of the parameter α versus ages of stars. Each point is the result of averaging of the parameter α over a given range of values. The vertical bars indicate the value of the weighted average value of the log t age variance, and the horizontal bars indicate the variance α in the averaged group. The groups have a number of stars from 2 to 13.

As can be seen from this diagram, in the whole the coefficient α is increasing versus age. Although the reliability of this distribution is not very high (see, for example, Soderblom 2014), in general, there is a tendency for the values of the parameter α to increase, which is an indirect argument in favor of an increase in the value of the far excess IR radiation with age. This result shows that, apparently, the amount of dust in the protoplanetary disks of young stars should increase during evolution.

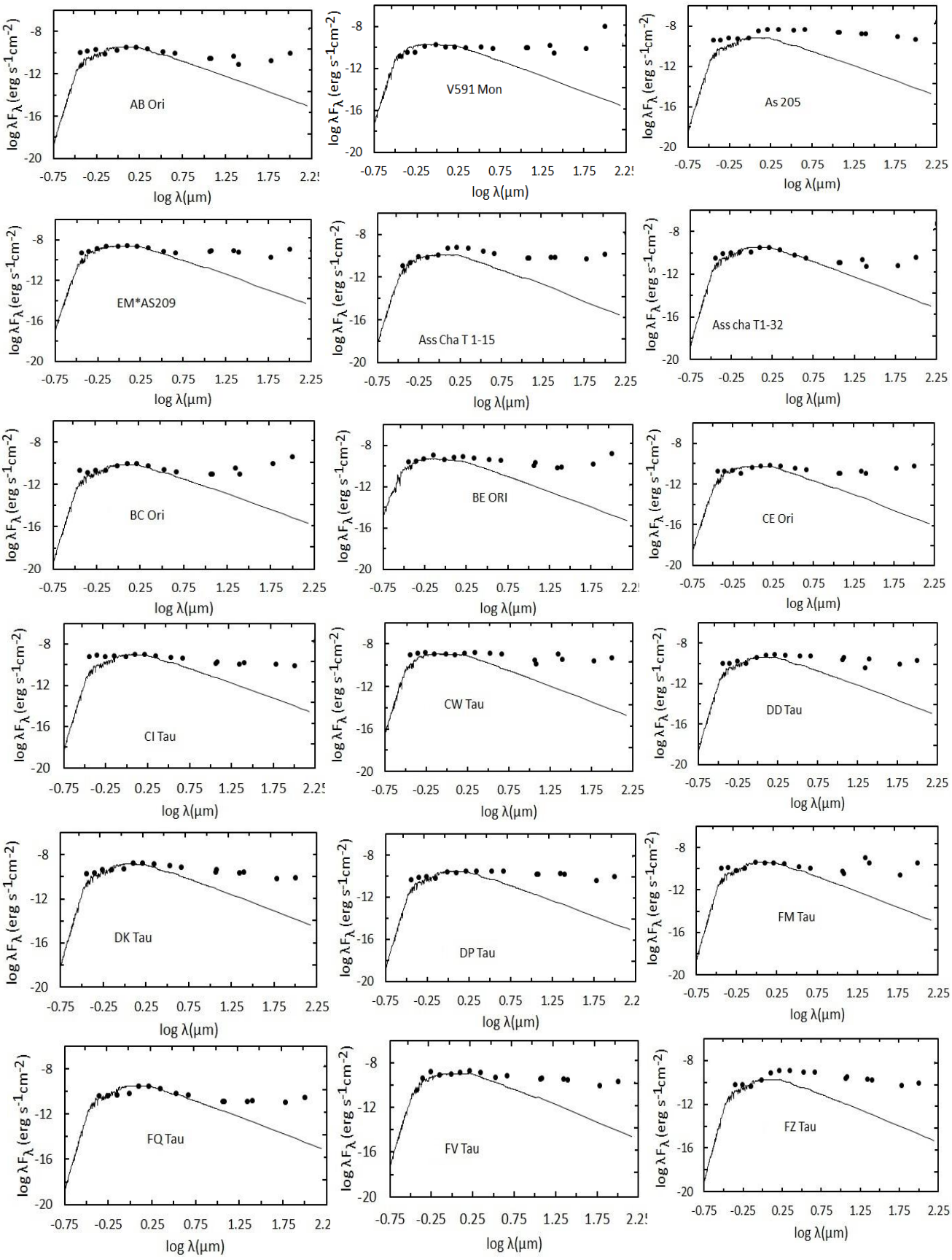

Figure 1: SED curves of program stars. Solid lines describe SEDs of standard star models by Castella and Kurucz (2004).

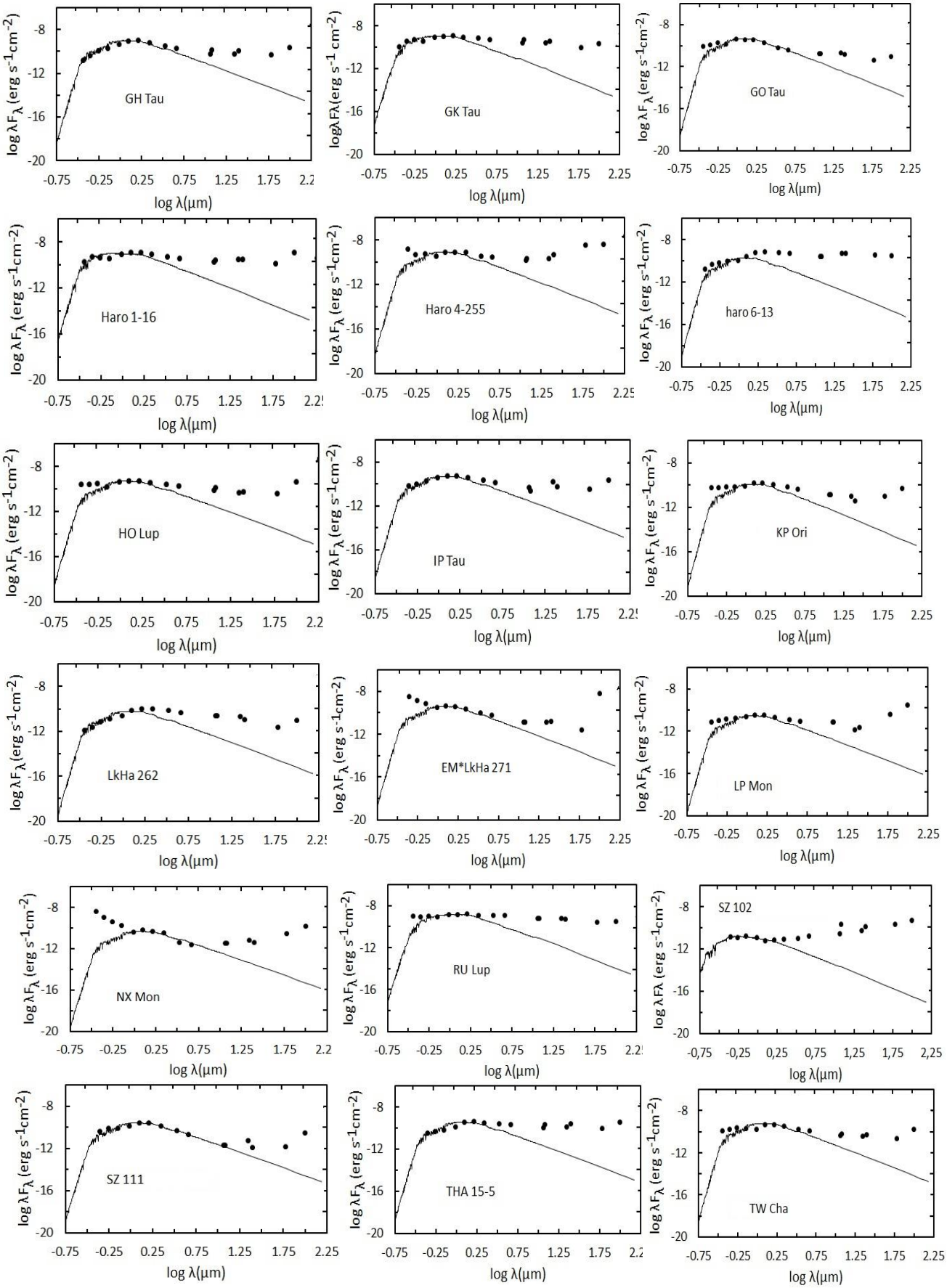

Figure 1 (Continued)

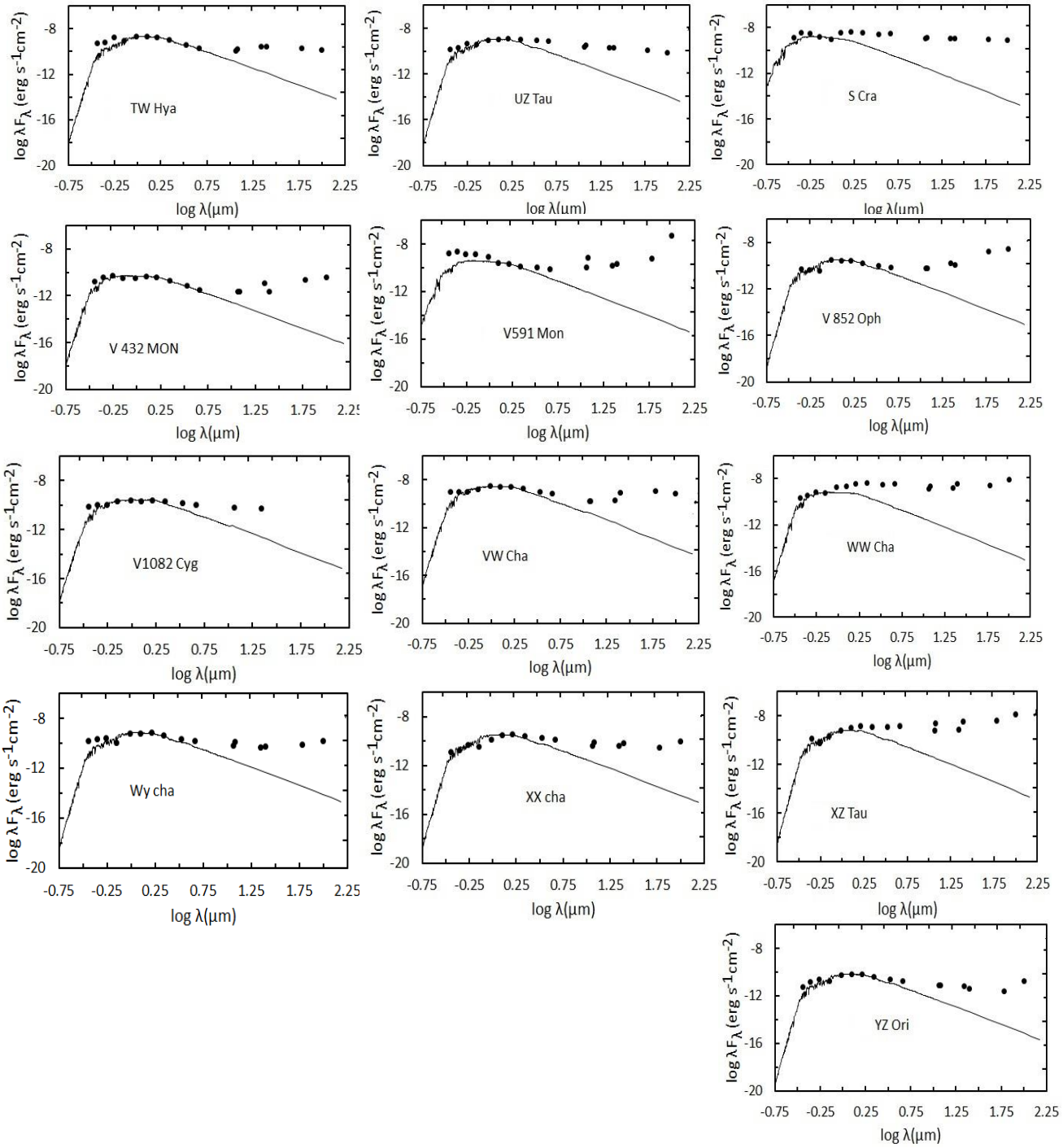

Figure 1 (Continued)

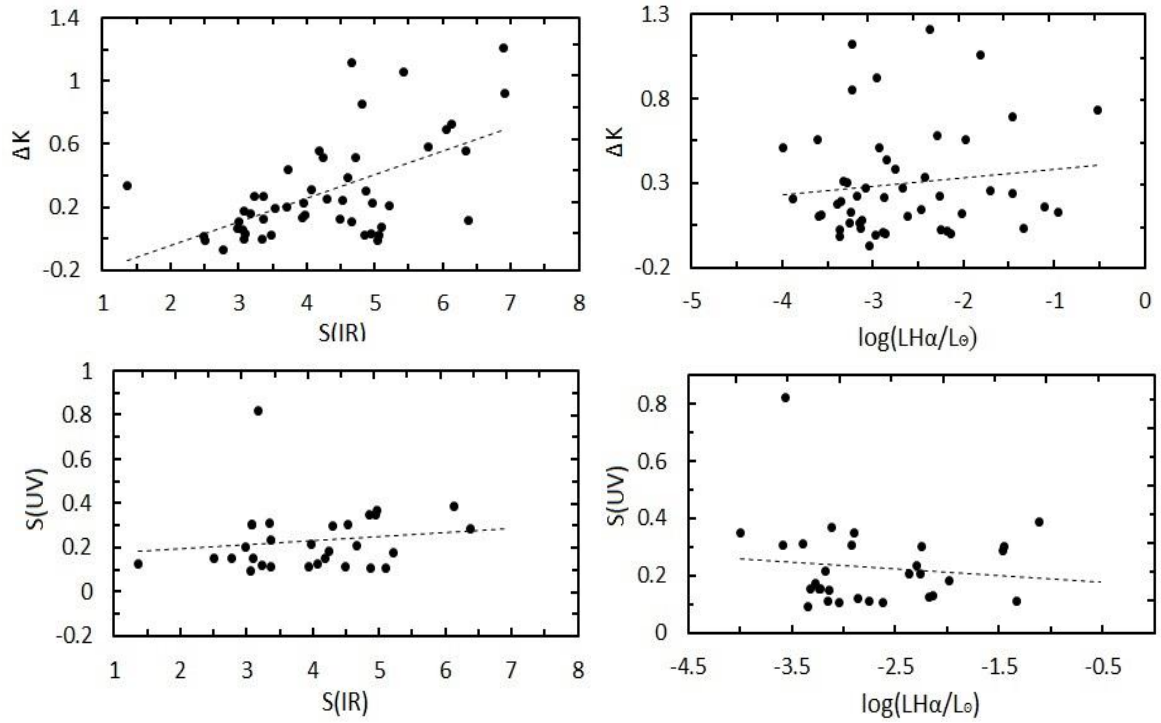

Figure 2: Diagrams of radiation excess parameters in the near (ΔK) ~ S(IR) far IR ranges, upper left panel, parameter ΔK and absolute luminosity in the Hα line, log (LHα) (top panel, right), between the parameters S(UV) ~ S(IR) bottom left, and S(UV) ~ log (LHα) – (bottom right panel). Dashed lines is linear regression.

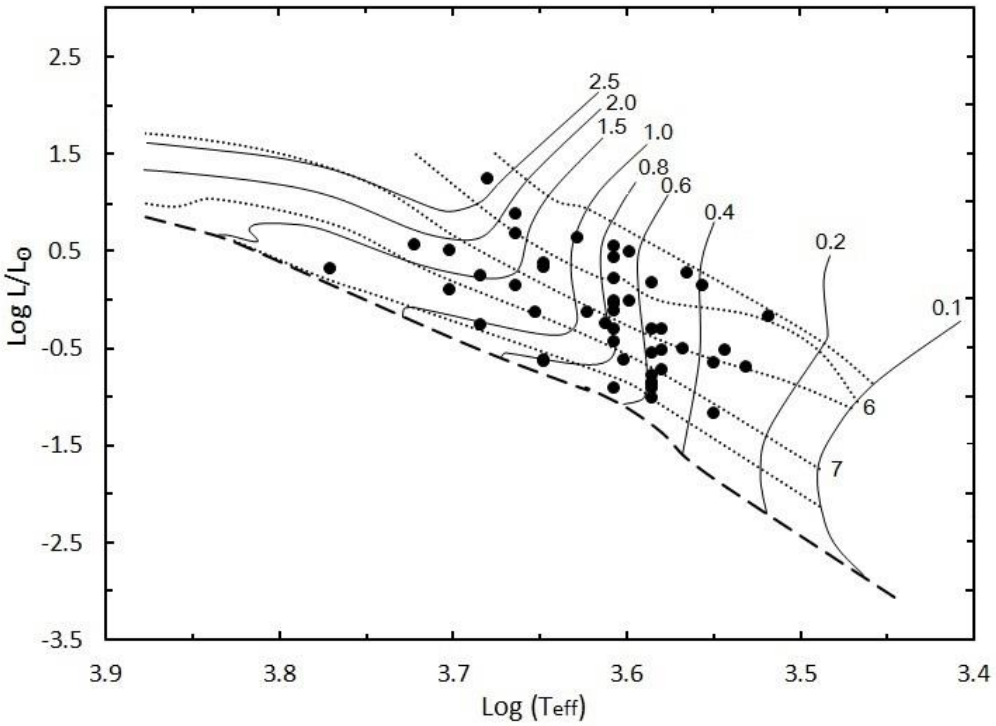

Figure 3: Location of program stars on the H-R diagram with evolutionary tracks according to Siess et al.(2000). The numbers on the solid lines indicate the masses, and near the dotted lines, the logarithms of the ages from 5.5 to 8 with a step of 0.5. The lower bold dotted line is the zero age line (ZAMS).

Table 2: The main parameters of program stars determined in this work

Target name	L*/L⊙	R/R⊙	M/M⊙	t, Myr	S(IR)	S(UV)	ΔK	type
LkHa 262	1.5	0.7	0.56	0.6	4.72		0.51	I
LkHα 271	7.9	3.0	1.8	0.6	4.94	0.35	0.03	II
FM Tau	0.2	0.5	0.6	15.8	3.94	0.11	0.13	II
CW Tau	1.8	0.7	1.5	5.6	4.19	0.15	0.55	II
DD Tau	0.7	0.8	0.3	0.3	4.24	0.18	0.51	II
DG Tau	0.5	1.2	0.75	5.0	3.08	0.31		II
DK Tau	0.9	2.9	0.73	5.0	3.24	0.12	0.27	II
XZ Tau	0.2	0.8	0.36	3.2	5.79		0.58	I
UZ Tau	1.4	3.1	0.4	0.5	3.36	0.23	0.27	II
VGH Tau	0.3	2.4	0.51	4.0	3.00		0.11	II
GK Tau	0.8	0.7	0.95	4.0	3.08	0.31	0.18	II
CI Tau	1.7	1.7	0.7	1.0	3.35	0.31		II
DP Tau	0.3	0.6	0.45	3.2	4.08	0.13	0.31	II
GO Tau	0.5	1.9	0.55	2.5	2.77	0.15		II
YZ Ori	0.4	2.7	0.8	7.9	5.10	0.11	0.08	II
KP Ori	0.1	0.8	0.6	25.1	4.97	0.37	0.23	II
AB Ori	3.6	1.0	0.7	0.5	4.67	0.21	0.11	II
CE Ori	0.2	1.4	0.8	39.8	4.87	0.10	0.31	II
BC Ori	0.2	1.7	0.75	35.5	5.22	0.17	0.21	II
BE Ori	3.7	0.4	1.75	6.3	6.06		0.69	II
Haro 4-255	15.4	4.7	2.7	0.32	4.53	0.30	0.24	II
LP Mon	1.0	0.8	0.72	5.6	6.37	0.29	0.11	II
NX Mon	0.1	1.3	0.36	15.8	3.18	0.82	0.16	II
V591 Mon	4.8	1.0	1.65	1.0	6.12	0.39	0.73	II
V 432 MON	2.2	2.2	1.25	1.8	5.07			II
RU Lup	2.7	2.9	0.7	0.6	4.29	0.30	0.26	II
V 852 Oph	0.1	1.3	0.59	31.6	5.05			II
Haro 1-16	0.6	0.7	1	25.1	4.60		0.39	II
AS209	1.4	1.0	1.4	4.0	3.36	0.11	0.12	II
S CrA	2.1	0.4	1.3	20.0	5.43		1.06	I
FQ Tau	0.2	0.7	0.3	3.2	3.47		0.02	II
IP Tau	0.2	4.3	0.52	10.0	3.71		0.20	II
FV Tau	2.4	2.5	1.25	1.6	3.72		0.44	II
Haro 6-13	0.1	1.6	0.95	25.1	4.81		0.85	I
FZ Tau	0.1	0.5	0.6	22.4	4.67		1.12	I
TW Cha	1.0	0.6	0.65	1.6	3.09	0.15		II
TW Hya	0.6	0.5	0.81	4.0	2.50	0.15		II
Ass Cha T1-15	0.2	0.9	0.75	63.1	6.91		0.92	II
WW Cha	1.3	2.1	1.3	12.6	6.90		1.21	II
Wy cha	0.8	2.6	0.72	2.5	2.99	0.20	0.07	II
VW cha	3.2	2.9	0.65	0.4	4.49	0.11	0.13	II
XX Cha	0.3	0.4	0.35	2.5	3.55		0.19	II
Ass cha T1-32	0.5	0.3	0.52	2.2	3.06	0.09		II
THA 15-5	0.1	0.8	0.7	50.1	3.96		0.23	II
HO Lup	1.9	0.8	0.45	0.4	3.98	0.21	0.15	II
SZ 102	0.1	0.4	1.8	5.0	6.34		0.56	I
SZ 111	0.3	0.5	0.59	5.0	2.49			II
AS 205	0.8	1.6	1.2	31.6	4.86	0.35		I
V 1082 Cyg	4.3	0.4	1	0.3	1.37	0.13	0.34	II

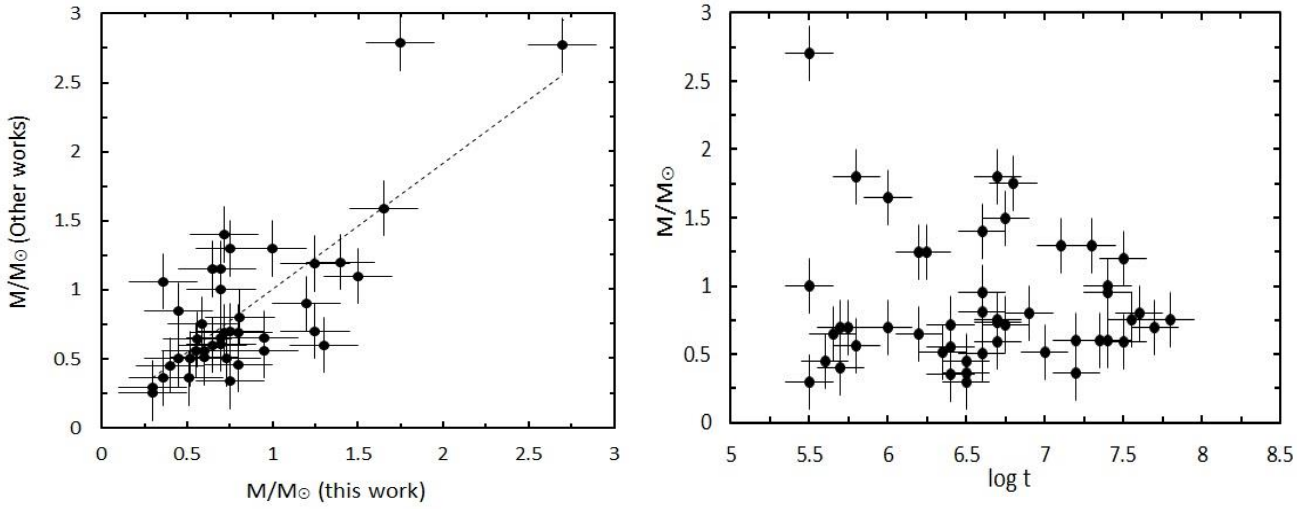

Figure 4: Comparison of the stellar masses obtained in this work with the data obtained in other works (left panel). The dotted line shows the linear approximation of the data. Vertical and horizontal bars shows the maximum error level. In the right panel, age-mass relation for program stars is presenting.

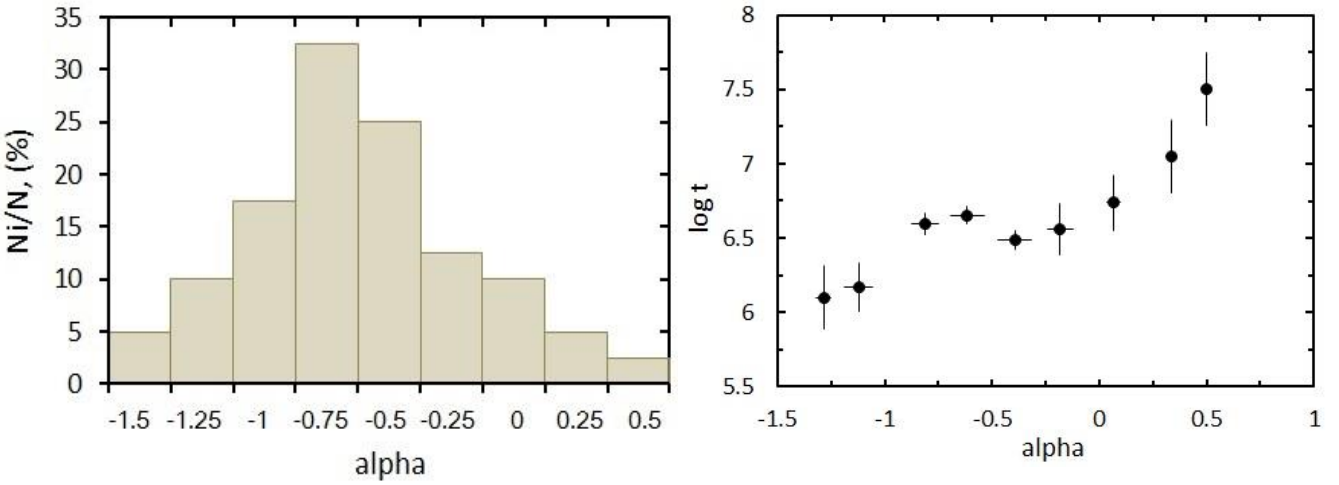

Figure 5: In the left panel, each step along the abscissa corresponds to the interval α for a given relative number of program stars Ni/N. The right panel shows the change in α with the age of the stars. Vertical and horizontal bars show the weighted average dispersion by parameters.

4. Conclusion

In this paper, we have studied the curves of the spectral energy distribution for 49 CTTS stars with variously developed emission lines in the spectrum. It is shown that in the set under consideration, all stars have a significant IR excess in the far IR range (10─100 μm). 30 of the selected program stars show a significant UV excess in the range of 0.36–0.70 μm. In addition, 39 stars exhibit excess emission in the near-IR range (2.2 μm) of the spectrum. As is known, the existence of UV excess radiation in CTTS is a consequence of the existence of disk accretion. It is obvious that in such disks the amount of gas is sufficient to support the accretion process. In addition to this, excess radiation in the near-IR range is also an argument in favor of the existence of gas accretion in the disk. Our data have shown that program stars often, but not always, have UV and ΔK excesses in their spectra simultaneously.

It was shown that only for 7 program stars the SED curve corresponds to type I, the remaining 42 objects have spectrum of type II. At the same time, no correlation is found between the UV and IR indicators of excess radiation. A correlation of about 52% between excess radiation in the near and far IR ranges was revealed. No correlation was found either with the luminosity in the Hα line and excesses in the UV and near IR ranges, which

indicates that different mechanisms are responsible for the emission of the Hα line.

We have determined the main parameters of the program stars. Comparison with literature data shows satisfactory agreement with the data obtained in other works. We have shown for the first time that the parameter α determined from relation (3) shows an increase with age. It is shown that with age, the amount of excess radiation in the far infrared range is increasing. Such a process is observed at least up the ages of 10 Myr.

The distribution diagram of the parameter α showed that the value of α is random, i.e. obeys the normal distribution law. At the same time, an increase in α (i.e., an increase in the excess in the far IR range) indicates an increase in dust in the disk with age.

References

Appenzeller I., Mundt R.: 1989, *Astron. & Astrophys. Rev.*, **1**, 291.

Bouvier J.P., Alencar S.H., Harries T.J., Johns-Krull M.C., Romanova M.M.: 2007, in *Protostars and Planets V*, ed. B. Reipurth, D. Jewitt, and K. Keil (Tucson, AZ: Univ. Arizona Press), 479.

Castelli F., Kurucz R.I.: 2004, ATLAS9, *https://www.user.oats.inaf.it/castelli/grids/*.

Corcoran M., Ray T.P.: 1998, *A&Ap*, **331**, 147.

Grankin K.N., Melnikov S.Yu., Bouvier J. et al.: 2007, *Astron. & Astrophys.*, **461**, 183.

Herbig G. H., Bell K. R.: 1988, *Lick Observ. Bull.*, **No 1111**.

Herbst W., She vchenko V.S.: 1999, *Astron. J.*, **118**, 1043.

Hughes A.M., Duchêne G., Matthews B.C.: 2018, *Ann. Rev. Astron. & Astrophys.*, **56**, 541.

Ismailov N.Z., Kholtygin A.F., Romanyuk I.I., Pogodin M.A.: 2021a, *Az. Astron. J.*, **16**, No 2, 5.

Ismailov N.Z., Kholtygin A.F., Romanyuk I.I., Pogodin M.A., Moiseeva A.V.: 2021b, *Astrophys. Bull.*, **76**, № 4, 415.

Ismailov N.Z., Valiyev U.S.: 2022a, *Astron. Rep.* (accepted for publication).

Jayawardhana R., Mohanty S., Basri G.: 2003, *Astrophys. J.*, **592**, 282.

Kenyon S.J., Hartmann L.: 1995, *Astrophys.J. Suppl. Ser*., **101**, 117.

Lada C.J.: 1987, *IAU Symposium*, **115**, 1.

Mamajek E.E.: 2009, in *AIP Conf. Ser. /*Eds. T.Usuda, M.Tamura, M.Ishii, **1158**, 3.

Manara C.F., Natta A., Rosotti G.P.: 2020, *A&Ap*, **639**, A58.

Pecaut M.J., Mamajek E.E.: 2013, *Astrophys.J.* Suppl.Ser. 208, 9.

Petrov P.P.: 2021, *Acta Astrophysica Taurica* 2, No 1, 1.

Pollack J. B., Hubickyj O., Bodenheimer P. et al.: 1996, *Icarus*, **124**, 62.

Ribas Á., Merín B., Bouy H., Maud L.T.: 2014, *A&Ap*, **561**, A54.

Siess L., Dufour E., Forestini M.: 2000, *A&Ap*, **358**, 593.

Soderblom D.R., Hillenbrand L.A., Jeries R.D., Mamajek E.E., Naylor T.: 2014, *Protostars Planets VI*, 219.

Strom K.M., Strom S.E., Edwards S. et al.: 1989, *Astron. J.*, **97**, 1451.

Villenave M., Ménard F., Dent W.R.F. et al.: 2021, *A&Ap*, **653**, A46.

Williams J.P., Cieza L.A.: 2011, *Ann. Rev. Astron. & Astrophys*., **49**, 67.

Wyatt M. C., Pani´c O., Kennedy G. M., Matrà L.: 2015, *Astrophys. & Spase Sci*., **357**, 103.